Threonine 150 Phosphorylation of Keratin 5 Is Linked to Epidermolysis Bullosa Simplex and Regulates Filament Assembly and Cell Viability

Mugdha Sawant[1], Nicole Schwarz[1], Reinhard Windoffer[1], Thomas M. Magin[2], Jan Krieger[3], Norbert Mücke[3], Boguslaw Obara[4], Vera Jankowski[5], Joachim Jankowski[5,6], Verena Wally[7], Thomas Lettner[7] and Rudolf E. Leube[1]

A characteristic feature of the skin blistering disease epidermolysis bullosa simplex is keratin filament (KF) network collapse caused by aggregation of the basal epidermal keratin type II (KtyII) K5 and its type I partner keratin 14 (K14). Here, we examine the role of keratin phosphorylation in KF network rearrangement and cellular functions. We detect phosphorylation of the K5 head domain residue T150 in cytoplasmic epidermolysis bullosa simplex granules containing R125C K14 mutants. Expression of phosphomimetic T150D K5 mutants results in impaired KF formation in keratinocytes. The phenotype is enhanced upon combination with other phosphomimetic K5 head domain mutations. Remarkably, introduction of T150D K5 mutants into KtyII-lacking (KtyII$^{-/-}$) keratinocytes prevents keratin network formation altogether. In contrast, phosphorylation-deficient T150A K5 leads to KFs with reduced branching and turnover. Assembly of T150D K5 is arrested at the heterotetramer stage coinciding with increased heat shock protein association. Finally, reduced cell viability and elevated response to stressors is noted in T150 mutant cells. Taken together, our findings identify T150 K5 phosphorylation as an important determinant of KF network formation and function with a possible role in epidermolysis bullosa simplex pathogenesis.

Journal of Investigative Dermatology (2018) **138,** 627–636; doi:10.1016/j.jid.2017.10.011

INTRODUCTION

Keratin intermediate filaments (KFs) constitute a major part of the epithelial cytoskeleton. They are obligatory heteropolymers of type I and type II keratin polypeptides. Each polypeptide consists of a conserved α-helical, approximately 310-amino acid–long rod domain that is flanked by variable amino-terminal head and carboxy-terminal tail domains (Herrmann and Aebi, 2016; Loschke et al., 2015; Pan et al., 2013). The significance of KFs for structural scaffolding of epithelia is evident from the skin fragility observed in the autosomal dominant blistering disease epidermolysis bullosa simplex (EBS), which is caused by mutations of the type II keratin (K) 5 or type I K14 (Coulombe and Lee, 2012; Homberg and Magin, 2014; Szeverenyi et al., 2008). KF collapse into cytoplasmic granules is a characteristic feature of EBS, especially upon mechanical and other types of stress (Beriault et al., 2012; Chamcheu et al., 2011; Homberg et al., 2015; Russell et al., 2004). A still unresolved conundrum is why EBS-mutant keratins are able to form perfect 10-nm filaments in vitro (Herrmann et al., 2002) and are often part of normal-appearing KF networks in EBS-derived keratinocytes (Beriault et al., 2012; Morley et al., 2003) and even in epidermis of EBS patients (Anton-Lamprecht, 1994). These observations suggest that the mutations are not responsible for the deficiency in filament formation on their own but require additional factors.

Keratin granules have also been described in the context of increased keratin phosphorylation (reviews in Sawant and Leube, 2017; Snider and Omary, 2014). Phosphorylation targets almost exclusively the head and tail domains of keratins (Gilmartin et al., 1980; Ikai and McGuire, 1983; Sawant and Leube, 2017; Snider and Omary, 2014; Steinert, 1988) with a preference for the head domain of type II keratins (Liao et al., 1995; Yano et al., 1991). Type II keratins share the conserved and unique sequence motif LLS/TPL in their H1 head subdomain, which is a major target for phosphorylation (Toivola et al., 2002). Moreover, the H1 subdomain is essential for normal KF assembly (Hatzfeld and Burba, 1994; Wilson et al., 1992), and mutations in this domain have been identified in EBS patients (www.interfil.org). Phosphorylation of non-epidermal keratins was linked to multiple cellular

[1]*Institute of Molecular and Cellular Anatomy, RWTH Aachen University, Aachen, Germany;* [2]*Institute of Biology and Translational Center for Regenerative Medicine, University of Leipzig, Leipzig, Germany;* [3]*Biophysics of Macromolecules, German Cancer Research Center, Heidelberg, Germany;* [4]*School of Engineering and Computing Sciences, Durham University, Durham, UK;* [5]*Institut für Molekulare Herz-Kreislaufforschung, RWTH Aachen University, Aachen, Germany;* [6]*School for Cardiovascular Diseases, Maastricht University, Maastricht, The Netherlands; and* [7]*EB House Austria, Research Program for Molecular Therapy of Genodermatoses, Department of Dermatology, University Hospital Salzburg, Paracelsus Medical University, Salzburg, Austria*

Correspondence: Rudolf E. Leube, Institute of Molecular and Cellular Anatomy, RWTH Aachen University, Wendlingweg 2, 52074 Aachen, Germany. E-mail: rleube@ukaachen.de

Abbreviations: EBS, epidermolysis bullosa simplex; FCS, fluorescence correlation spectroscopy; K, keratin; KF, keratin filament; KtyII, basal epidermal keratin type II; MTT, 3-(4,5-dimethylthiazol-2-yl)-2,5-diphenyltetrazolium bromide; ULF, unit length filament; WT, wild type

Received 4 July 2017; revised 11 September 2017; accepted 8 October 2017; accepted manuscript published online 6 December 2017

dysfunctions in the context of diseases affecting the liver (Guldiken et al., 2015; Ku et al., 1998; Stumptner et al., 2000; Zatloukal et al., 2000), pancreas (Liao and Omary, 1996), and colon (Zhou et al., 2006). Whether phosphorylation of epidermal keratins has similar effects on cellular physiology has not been examined in much detail.

The aim of this study was to resolve a potential link between EBS mutations, the occurrence of phosphorylation, and cellular physiology. Considering the shortcomings of other approaches such as the lack of specificity in drug-induced changes in phosphorylation (Feng et al., 1999; Liao et al., 1997) or the limited meaning of in vitro studies for the in vivo situation (Deek et al., 2016; Herrmann et al., 2002), we used a mutation-based strategy to investigate the effect of phosphorylation in the keratin type II head region in living cells.

RESULTS AND DISCUSSION

Phosphorylation of threonine 150 of K5 is linked to keratin aggregation in generalized severe EBS

It has been suggested that keratin phosphorylation is involved in granule formation of mutant keratin in EBS (Chamcheu et al., 2011; Woll et al., 2007). To directly test whether keratin phosphorylation is linked to granule formation, immunolocalization of keratin phosphoepitopes was performed on immortalized EBDM-4 keratinocytes carrying an R125C K14 mutation. The cells were derived from a patient with generalized severe EBS, previously referred to as Dowling Meara-type EBS (Fine et al., 2014). Using an antibody recognizing the T150 phosphoepitope of the conserved LLS/TPL sequence motif in the type II keratin K5 (Toivola et al., 2002) the strongest immunoreactivity was detected in granules (Figure 1b). Much weaker reactivity was seen in thick keratin filament bundles and only very weak to no reactivity was noted in thin filaments, as was the case in wild-type (WT) control keratinocytes of line hKC (Figure 1a and b). The fluorescence intensity patterns of the phosphoepitope-specific antibodies differed significantly from those observed with antibodies detecting keratins, irrespective of their phosphorylation status, which stained keratin bundles and granules at similar intensity and also clearly detected thin filaments (Figure 1a and b). Expression of YFP-tagged R125C K14 mutants in immortalized HaCaT keratinocytes also showed an enrichment of the T150 K5 phosphoepitopes in cytoplasmic granules (Figure 1c). Taken together, we conclude that T150 K5 phosphorylation is increased in granules that are formed in the presence of EBS mutant keratins. Immunoblotting of whole-cell lysates showed that the total level of K5 was reduced to 56% in EBDM-4 cells compared with hKC cells and that the ratio of phosphorylated to total K5 was approximately 1.5 times increased (see Supplementary Figure S1 online). The reduced level of keratins may be a consequence of increased keratin dynamics coupled with keratin degradation (Loffek et al., 2010; Werner et al., 2004; Windoffer et al., 2011).

Phosphomimetic keratin type II head domain mutations lead to increased granule formation in the presence of WT keratins

To delineate the potential role of T150 K5 phosphorylation in EBS skin fragility, the impact of phosphomimetic keratin mutation on KF network organization was studied. To this end, YFP-tagged WT K5 and phosphomimetic T150D K5 mutants were transfected into HaCaT keratinocytes. In both instances, a typical KF network was detected in most transfected cells, although granules were frequently observed next to KFs (Figure 2a and b). In some instances, the KF network was completely disrupted, leaving only granules (Figure 2c). Quantitation showed a slight decrease in the filament-only phenotype for the phosphomimetic mutant which was, however, statistically not significant (76% vs. 65%) (Figure 2d).

In addition to T150, multiple other potential phosphorylation sites are present in the K5 head domain (see Supplementary Figure S2a online and PHOSIDA database). To find out whether these other phosphorylation sites exacerbate the T150D-induced perturbation of KF network formation, further expression constructs were prepared containing the T150D mutation in all possible combinations with four other phosophomimetic mutations resulting in four double, six triple, four quadruple, and one quintuple mutants, which were transfected into HaCaT cells. Quantitative assessment showed that increasing the number of phosphomimetic sites correlated in general with a further decrease of the filament-only phenotype, suggesting that KF network formation was increasingly impaired (Figure 2d). Despite this overall tendency, certain sites had little effect or even improved the KF-network formation in some combinations (e.g., S35, S76).

To test whether the observed effects also apply to other keratins, we produced and tested a complementary set of mutants for the type II K8 (Figure 2e and see Supplementary Figure S2b and c). In this case, the phosphomimetic mutation S73D in the conserved LLS/TPL sequence motif was combined with four other phosphomimetic mutations of the head domain, again in all possible combinations. Transfection of the corresponding CFP-tagged fusion proteins showed very similar effects to those observed for K5.

Our observations in cultured cells are supported by published in vitro observations that showed that increasing the ratio of phosphomimetic K8 mutants to WT K8 reduces KF network connectivity (Deek et al., 2016). They are also in accordance with the observation that the impairment of in vitro KF assembly was proportional to the size of deletion in the K8 head domain (Hatzfeld and Burba, 1994).

Phosphomimetic T150 K5 mutation prevents keratin network formation in the absence of WT keratins

The low degree of phenotypic penetrance of the phosphomimetic mutants in HaCaT transfectants suggested that the phenotype was masked by endogenous WT keratins. This prompted us to use murine epidermis-derived keratinocytes lacking type II keratins (KtyII$^{-/-}$) (Kroger et al., 2013). Although WT K5 YFP and phosphomimetic T150D K5 YFP both integrated into the typical endogenous KF network of WT control keratinocytes, only K5 YFP was able to induce KF network formation in KtyII$^{-/-}$ cells, whereas T150D K5 YFP was not (Figure 2f, g, i, and j). Instead, strong diffuse fluorescence was detectable in the cytoplasm of all T150D K5 YFP-transfected KtyII$^{-/-}$ cells. In addition, small granules were visible throughout the cytoplasm. Occasionally, filamentous structures were seen in the cell periphery (Figure 2j).

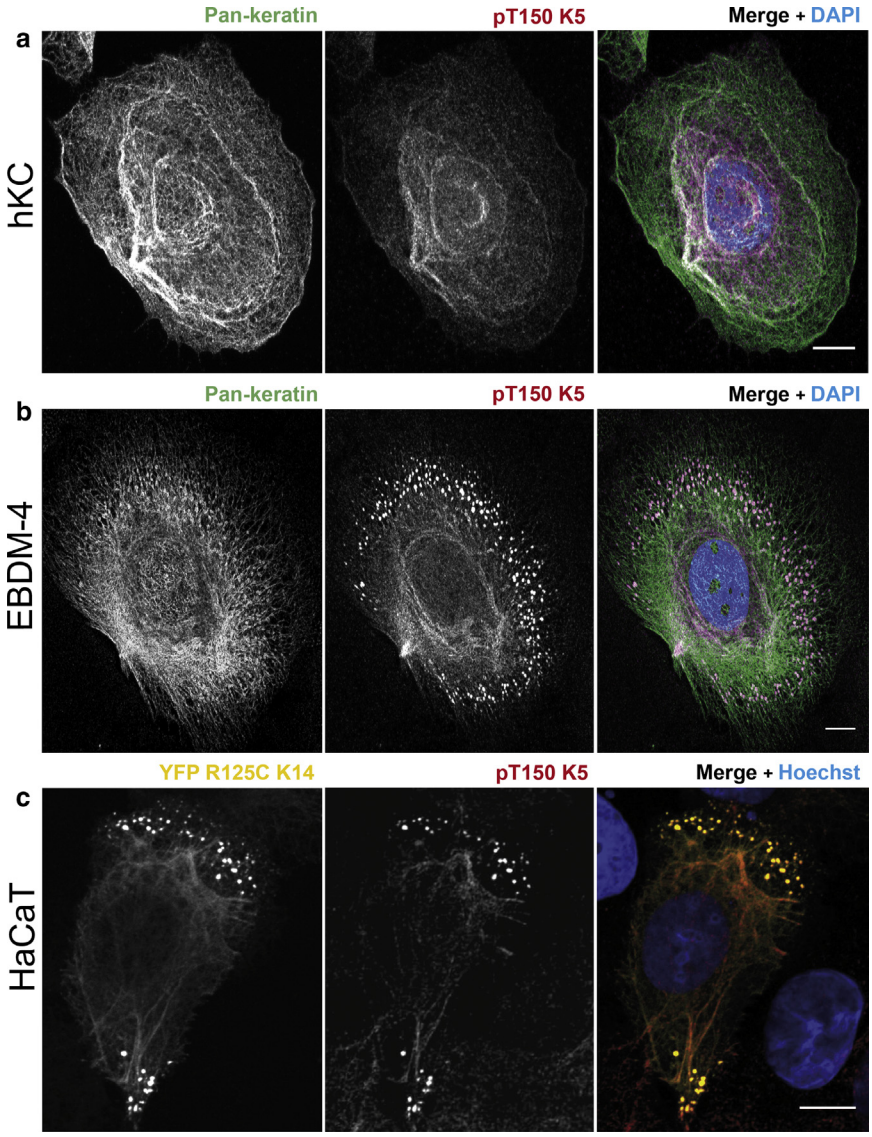

Figure 1. Phosphorylated threonine 150 K5 (pT150 K5) epitopes are enriched in cytoplasmic keratin granules of generalized severe EBS-derived keratinocytes. (**a**) Pan-keratin antibody staining shows normal KF network in keratinocytes derived from a healthy individual (hKC), whereas (**b**) KF reduction and abundant keratin granules are present in generalized severe EBS-derived EBDM-4 cells and also in (**c**) epidermal HaCaT cells, producing YFP R125C K14 mutants. Counterstaining with antibody LJ4 recognizing pT150 K5 shows weak reactivity of KF bundles in (**a**) hKC (middle panel) and (**b**) most prominent staining of granules in EBDM-4 (middle panel) and (**c**) YFP R125C K14-producing HaCaT cells (corresponding merged images with nuclear DAPI stains in **a**–**c,** right panels). Scale bars = 10 μm. EBS, epidermolysis bullosa simplex; K, keratin; KF, keratin filament.

Obviously, the additional negative charge at the single T150 position in the K5 H1 head domain was sufficient to completely prevent KF network formation in the absence of WT type II keratins. In contrast, phosphorylation-deficient T150A K5 YFP mutants formed a KF network in the WT and KtyII$^{-/-}$ background, although KF bundling appeared to be enhanced (Figure 2h and k).

To further analyze the phenotypes of T150 K5 mutants, stable clones were prepared for T150D and T150A K5 mutants, and WT K5 (Figure 2l–p). They presented the same features as transient transfectants. Some variability in the number of granules was noted for the T150D K5 YFP mutant. The peripheral filamentous structures of T150D K5 YFP were seen starting only at 10 days after seeding.

Mutation of T150 in K5 affects keratin dynamics

Time-lapse imaging was performed to examine dynamic properties of the T150D and T150A K5 YFP in KtyII$^{-/-}$ keratinocytes. A direct comparison of both mutants to WT K5 YFP is shown in Supplementary Movie S1 online. In T150D K5 YFP keratinocytes, diffuse keratin fluorescence predominated in the cytoplasm. In addition, very small fluorescent dots were detected moving at random throughout the cell. Several of the brightest dots were seen at the tips of cell protrusions. They were short-lived and had an overall tendency to move inward. In T150A K5 YFP keratinocytes, small particles were generated in the cell periphery. They grew, while moving toward the cell interior, where they integrated into the KF network. These features have been described as part of the keratin cycle of assembly and disassembly (Windoffer et al., 2011).

Next, fluorescence recovery after photobleaching analyses were performed. As expected, fluorescence recovery was fastest (>50% within 1 minute) for T150D K5 YFP keratinocytes (Figure 3a and b). At longer time scales, reduced fluorescence recovery was detectable in T150A K5 YFP cells compared with K5 YFP cells (Figure 3c and d). Quantitative image analysis of segmented T150A K5 YFP-containing KF networks further showed that the mean filament length between two branching points was

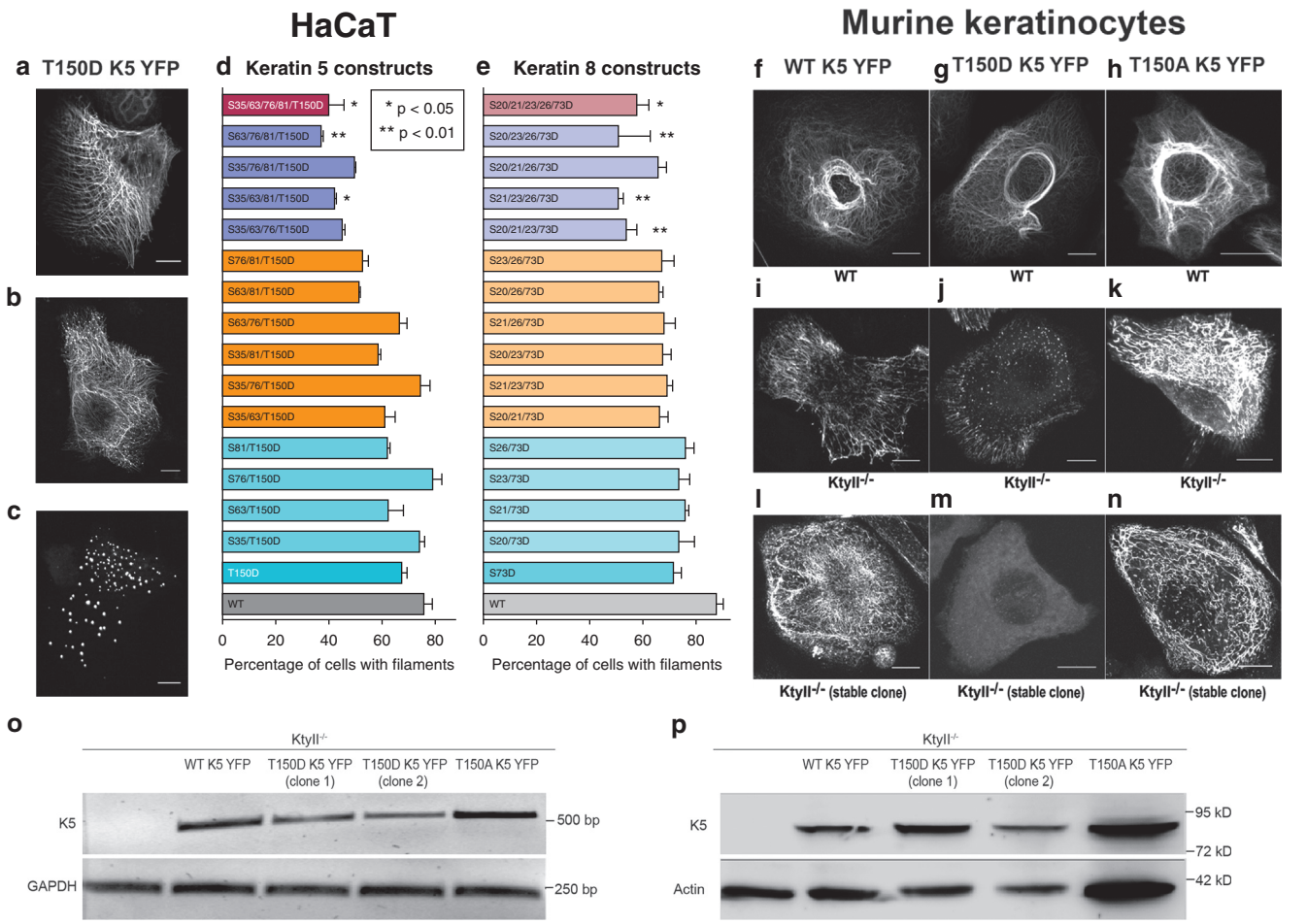

Figure 2. Phosphomimetic keratin head domain mutations alter KF network formation. Fixed HaCaTs expressing T150D K5 YFP show (**a**) filamentous, (**b**) filamentous plus granular, and (**c**) granular keratin. (**d, e**) The histograms show that cells with filamentous-only phenotype decrease with increasing phosphomimetic mutations in the K5 and K8 head domain. n = 200/construct/experiment; triplicate experiments; Kruskal-Wallis analysis of variance and Dunn posttest. Error bars show mean ± standard deviation. (**f**–**n**) fluorescence microscopy of live murine WT and KtyII$^{-/-}$ keratinocytes expressing the indicated keratins (**f**–**k**) transiently or (**l**–**n**) stably. Note that T150D mutation prevents network formation, whereas T150A mutation increases network coarseness. Scale bars = 10 μm. (**o**) Reverse transcriptase-PCR and (**p**) immunoblots of lysates from WT keratin- and mutant keratin-expressing KtyII$^{-/-}$ cells showing similar keratin mRNA and protein levels. bp, base pair; K, keratin; KF, keratin filament; KtyII, basal epidermal keratin type II; WT, wild type.

significantly increased (see Supplementary Figure S3 online).

Phosphomimetic T150D K5 mutants accumulate as soluble heterotetramers, which show increased heat shock protein association

We next wanted to biochemically define the assembly/disassembly intermediates that are enriched in T150D K5 YFP keratinocytes. Therefore, the high salt-extractable soluble and high salt-resistant insoluble cell fractions were analyzed for the presence of K5 by immunoblotting. Figure 4a shows that, in contrast to KtyII$^{-/-}$ cells producing WT K5 YFP and T150A K5 YFP, approximately 70% of K5 was detected in the soluble pool of T150D K5 YFP KtyII$^{-/-}$ keratinocytes. To characterize the soluble pool in situ, cells were treated with Triton X-100 (Sigma-Aldrich, St. Louis, MO). This resulted in loss of the diffuse cytoplasmic fluorescence and unmasking of cytoplasmic granules (Figure 4b). We suggest that the diffuse fluorescence corresponds to the soluble pool and the granules to the insoluble pool.

Next, we wanted to determine the molecular nature of the diffuse T150D K5 species. To this end, we used fluorescence correlation spectroscopy (FCS). FCS is a microscopic technique that provides information on the local concentration and diffusion of fluorescently labeled proteins. In FCS one records the fluctuations of the fluorescence intensity from a tiny measurement volume defined by the focal volume of the microscope with high temporal resolution (micro- to milliseconds). These fluctuations are caused by fluorescing particles entering and leaving the observation volume and thus carry information about the motion of these particles. To extract mobility parameters of the fluorophores, the intensity time traces are evaluated using a temporal autocorrelation analysis, which yields FCS correlation curves. Finally, the mobility parameters are extracted by fitting mathematical models representing different experimental conditions (Elson and Magde, 1974).

We used single-plane illumination microscopy-based FCS as an extension of the FCS technology, which measures FCS curves not only at a single spot at a given point in time but at

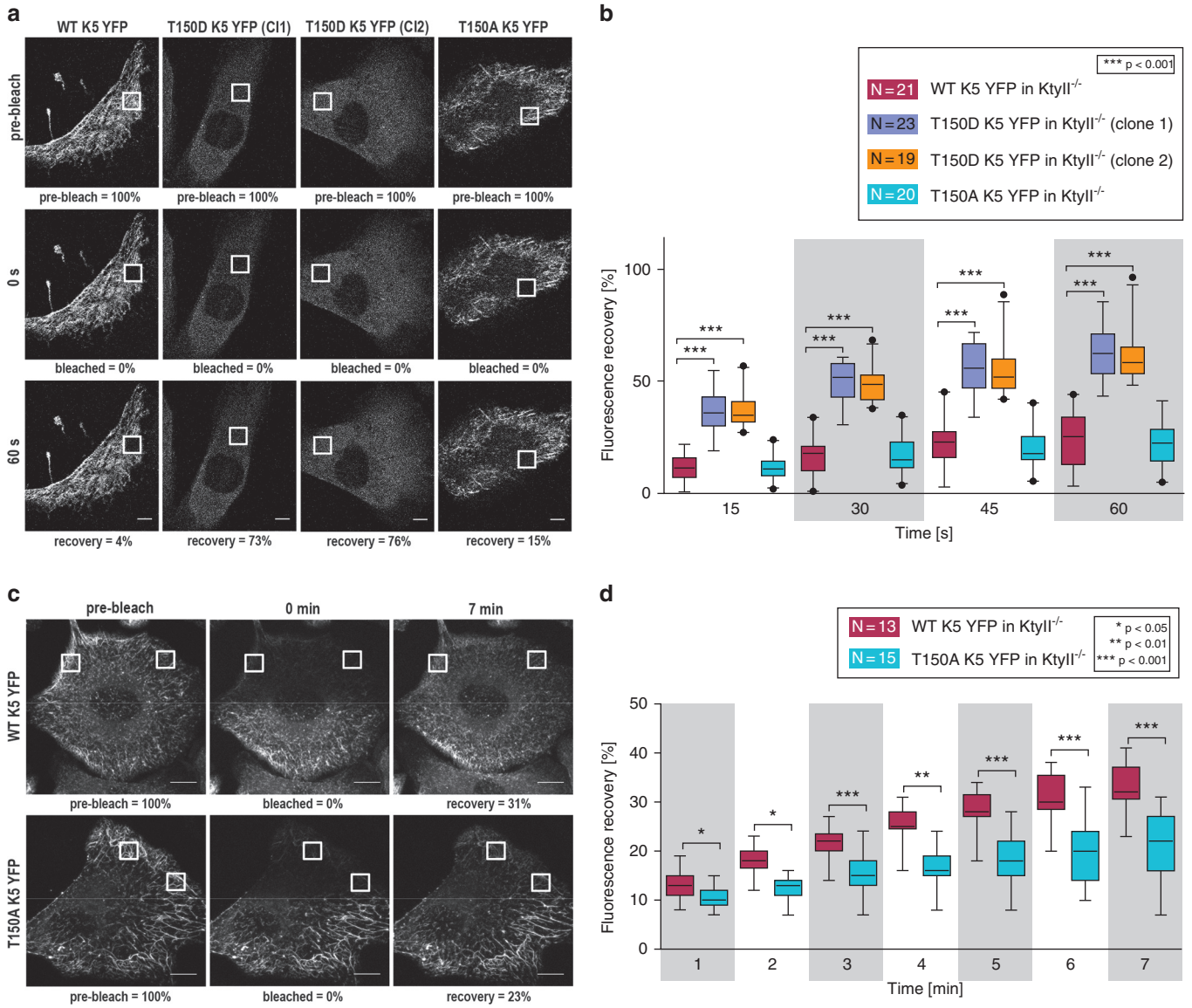

Figure 3. T150 K5 phosphorylation regulates keratin dynamics. FRAP analyses were performed in stably transfected KtyII$^{-/-}$ cells. Regions selected for quantitation are demarcated by squares. (**a, b**) The images shown were recorded 60 seconds before bleaching (pre-bleach), immediately afterward (0 seconds), and after 60 seconds. Phosphomimetic T150D K5 YFP has a much higher fluorescence recovery than WT K5 YFP and phosphorylation-deficient T150A K5 YFP. Statistical analysis was performed with Kruskal-Wallis analysis of variance followed by Dunn posttest. (**c, d**) Bleached and unbleached regions are separated by horizontal lines. Quantitation shows that T150A K5 YFP KFs have a lower turnover than WT K5 YFP KFs. Statistical analysis was done with Mann-Whitney test. Scale bars = 10 μm. Whiskers are 5th–95th percentiles. FRAP, fluorescence recovery after photobleaching; K, keratin; KtyII, basal epidermal keratin type II; min, minute; s, second; WT, wild type.

thousands of different locations simultaneously within an arbitrarily positionable 1- to 3-μm–thick plane (Krieger et al., 2015; Wohland et al., 2010). We were able to determine mobility parameters of labeled keratin particles with the help of single plane illumination microscopy-FCS in live cells, even when abundant filaments or granules were present. This was achieved during postprocessing of the measurements by selecting mobility parameters from filament- and granule-free regions within the observation plane. The FCS-correlation curves from these selected pixels were evaluated with a model that represents a mixture of two diffusing species (*slow* and *fast*) that best describes the data in an interpretable way in live-cell FCS while not overfitting it (Dross et al., 2009; Sun et al., 2015). Typically, the fast diffusing component can be interpreted as more or less freely diffusing small particles. The slowly diffusing component is typically interpreted to represent a combination of several effects in the complex environment of the cell: hindered (anomalous) diffusion, motion of larger structures inside the cell (that fluorophores stick to), and reorganization/motion of the entire cell. As expected, our measurements showed a fast and a slow component. The slow component showed diffusion coefficients that were universally in the range of $D_{slow} \approx 0.2–0.4$ μm^2/second and can be interpreted as suggested. The diffusion coefficients of the fast diffusing pool ($D_{fast} \approx 23.1 \pm 7$ μm^2/second for WT K5 YFP; $D_{fast} \approx 19.8 \pm 7$ μm^2/second and $D_{fast} \approx 19.8 \pm 4$ μm^2/second for T150D K5 YFP clones 1 and 2, respectively; $D_{fast} \pm$ standard deviation, n = 20 cells) were not significantly different

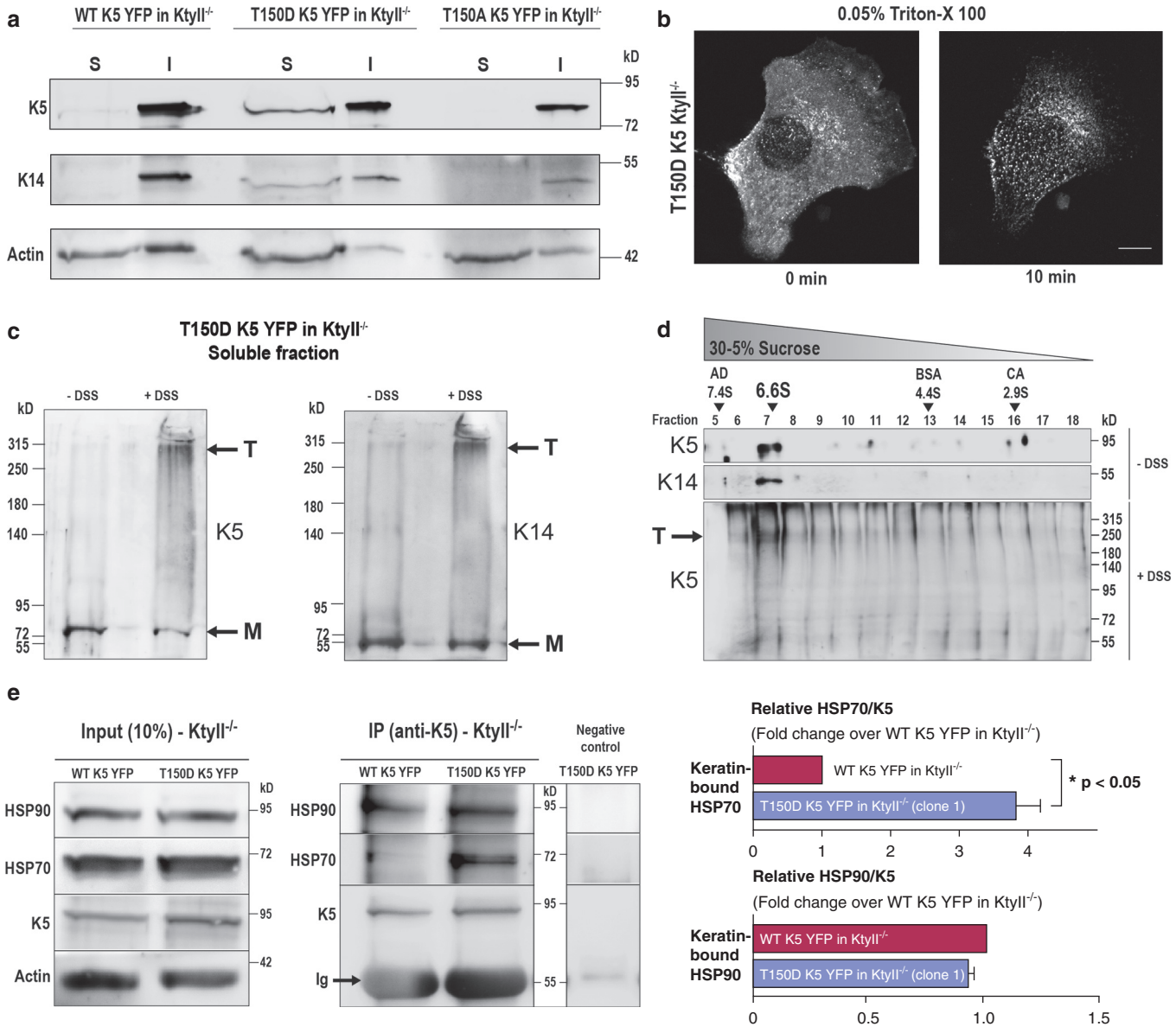

Figure 4. Phosphomimetic mutation of T150 K5 arrests KF assembly at the tetramer stage. (**a**) Immunoblots of soluble (S) and insoluble (I) extracts of KtyII$^{-/-}$ keratinocytes show increased solubility of T150D K5 YFP. (**b**) Imaging of T150D K5 YFP before and after Triton X-100 (Sigma-Aldrich, St. Louis, MO) treatment. Scale bar = 10 μm. (**c**) Immunoblots of T150D K5 YFP KtyII$^{-/-}$ soluble fraction with or without DSS-crosslinking show K5 and K14 monomers (M) and K5/K14 heterotetramers (T). (**d**) Immunoblots detecting K5 and K14 in density gradient fractions with and without DSS crosslinking. (**e**) Immunoblots of total cell lysates and K5 immunoprecipitates (quantification at right; n = 4) detecting HSP70 and HSP90. Statistical analysis was done with Mann-Whitney test. Error bars: mean ± standard deviation. AD, alcohol dehydrogenase; BSA, bovine serum albumin; CA, carbonic anhydrase; DSS, disuccinimidyl suberate; K keratin; KF, keratin filament; KtyII, basal epidermal keratin type II; min, minute; WT, wild type.

between the different keratin-expressing cell lines. From the measured diffusion coefficients and a calibration measurement of cells expressing unbound YFP ($D_{fast} \approx 27 \pm 8$ μm^2/second, n = 20), a hydrodynamic radius of approximately 9.3 nm was derived for WT K5 YFP and of approximately 10.9 nm for the T150D K5 YFP mutants. Assuming a cylindrical shape and taking length/diameter values for dimer, tetramer, and unit length filament (ULF) forms of keratin assembly intermediates into account (Herrmann et al., 1999; Quinlan et al., 1986), the soluble keratins are most likely tetrameric (for hydrodynamic radii of vimentin assembly intermediates see [Lopez et al., 2016]). The nonsignificant difference between the different keratin variants suggests that the molecular nature of the non-filamentous keratin pool was unaltered upon phosphomimetic mutation of T150.

To further corroborate our interpretation of the fast FCS-component, crosslinking experiments were performed. Disuccinimidyl suberate-mediated chemical crosslinking of soluble T150D K5 YFP led to formation of an approximately 280-kD K5- and K14-positive species corresponding to the expected size of K5 YFP/K14 tetramers (2 × 88 kD for K5 YFP and 2 × 54 kD for K14) (Figure 4c). Additionally, sucrose density gradient ultracentrifugation of soluble T150D K5 YFP was carried out. The K5-positive fractions had a Svedberg coefficient ($s_{20,w}$) of approximately 6.6 S (Figure 4d), in line with 4.7 S reported for the smaller K8/K18 tetramer (2 × 54 kD

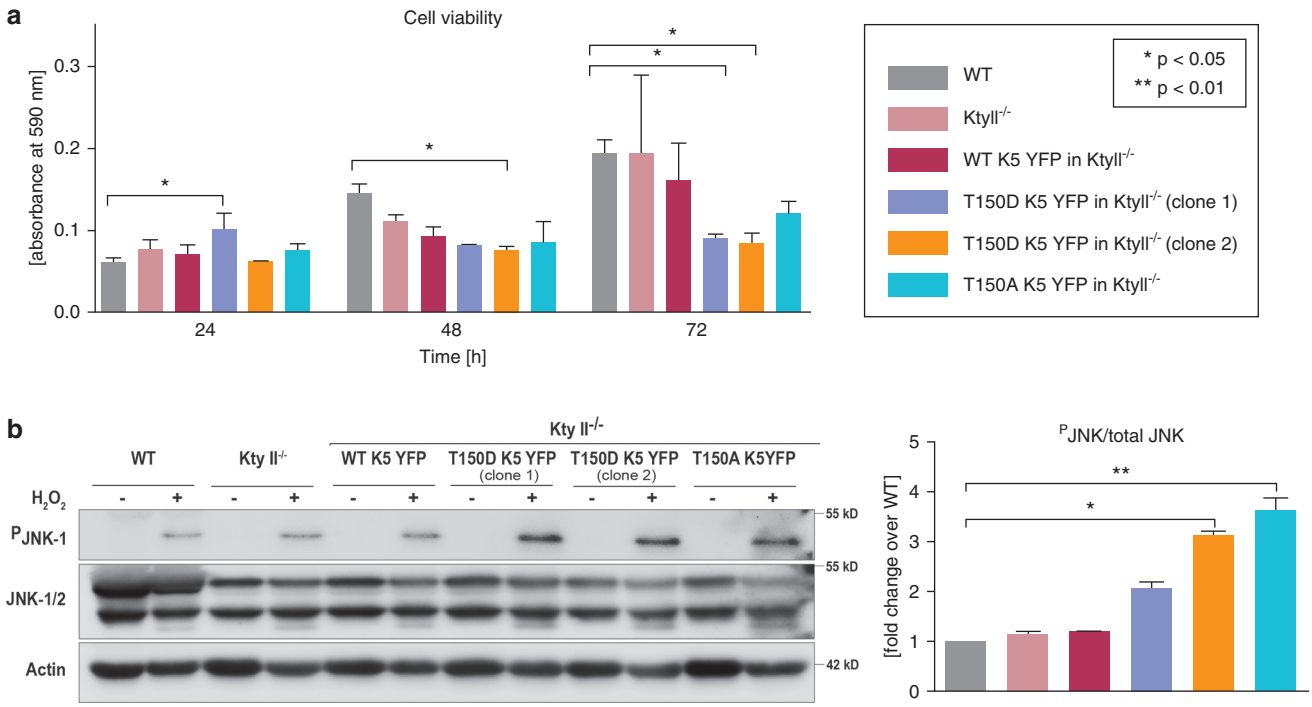

Figure 5. Mutation of T150 K5 alters cell viability and oxidative stress response. (**a**) MTT assay showing reduced cell viability of KtyII$^{-/-}$ cells stably expressing T150D K5 YFP and T150A K5 YFP compared with WT, KtyII$^{-/-}$, and WT K5 YFP KtyII$^{-/-}$ cells at different times after seeding. The experiment was replicated thrice, and each cell line was measured in triplicate. (**b**) Immunoblot showing up-regulation of phospho-JNK-1 (T183/Y185) in KtyII$^{-/-}$ cells stably expressing T150D K5 YFP and T150A K5 YFP compared with WT, KtyII$^{-/-}$, and WT K5 YFP KtyII$^{-/-}$ keratinocytes in response to H_2O_2-induced oxidative stress (10 mmol/L, 1 hour). Densitometric analysis of the phospho-JNK to total JNK ratio is shown at right. n = 3; statistical analysis by Kruskal-Wallis analysis of variance and Dunn posttest. Error bars: mean ± standard deviation. h, hour; K, keratin; KtyII, basal epidermal keratin type II; MTT, 3-(4,5-dimethylthiazol-2-yl)-2,5-diphenyltetrazolium bromide; WT, wild type.

for K8 and 2 × 48 kD for K18) (Chou et al., 1993; Lichtenstern et al., 2012). As expected, the peak fractions contained K14 that could be cross-linked to K5 (Figure 4d).

To examine whether the assembly arrest coincides with specific protein association, we performed immunoprecipitation experiments. HSP70-1A, HSP70-1B, HSP90-B1, and HSP105 were identified by mass spectrometry with Mascot scores of 60, 59, 74, and 56, respectively. Immunoblots showed that the total levels of the heat shock proteins were unaffected in the mutant cell lines (Figure 4e and data not shown). The amount of HSP70 bound to T150D K5 was elevated compared with the WT (Figure 4e, and for association of the K5 head domain and HSP70 see also Planko et al., 2007).

The observed assembly dysfunction of T150D K5/K14 tetramers may be a consequence of electrostatic repulsion between the negatively charged head domains of the T150D K5 mutant or defective staggering of the T150D K5/K14 tetramers and/or higher polymers. This may impair proper ULF formation or lead to reduced stability of ULFs. The increased heat shock protein association can be taken as an indication of altered spatial arrangement of the early assembly intermediates.

Mutation at T150 K5 reduces cell viability and up-regulates JNK signaling

To test the consequences of T150 mutation for cell physiology, cell viability was examined by 3-(4,5-dimethylthiazol-2-yl)-2,5-diphenyltetrazolium bromide (MTT) assay. Figure 5a shows that both T150D K5YFP cell clones had significantly reduced cell viability 72 hours after seeding. In addition, a slight reduction in cell viability was noted for T150A K5 YFP cells. To find out whether the reduced cell viability is linked to increased cellular sensitivity to stress, we examined the oxidative stress response in the KtyII$^{-/-}$-derived cell clones using H_2O_2. Both T150D K5YFP and T150A K5YFP cells presented increased JNK signaling compared with WT controls (Figure 5b). ERK and p38 MAPK signaling, however, were not significantly altered (see Supplementary Figure S4 online). Elevated MAPK signaling and increased susceptibility to stress were also reported for generalized severe EBS (Chamcheu et al., 2011; Wagner et al., 2013; Wally et al., 2013). Moreover, the presence of mutant keratin granules lower the threshold for inducing the unfolded protein response, which is often coupled with altered mitochondrial function, leading to oxidative stress (Malhotra and Kaufman, 2011; Senft and Ronai, 2015).

OUTLOOK/CONCLUSIONS

The scheme in Figure 6 summarizes the situations encountered in the different cellular scenarios examined in this study and relates them to the different assembly stages of keratin network formation. It highlights the importance of the end domains, especially in higher-order structures. It has been emphasized that the rod domains are crucial for coiled-coil formation of the parallel heterodimers and subsequent antiparallel, staggered alignment of heterodimers into nonpolar tetramers with little or no influence of the protruding, mostly unstructured head and tail domains (cf. (Guzenko et al.,

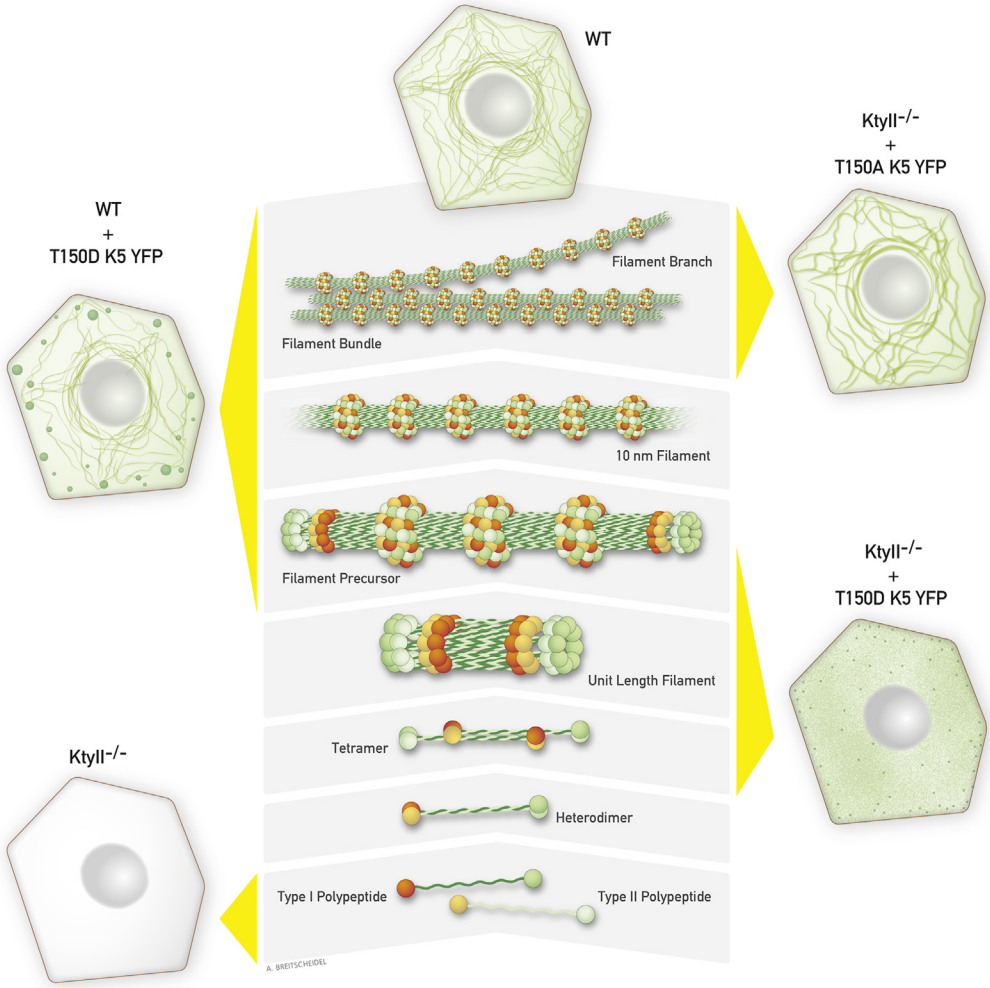

Figure 6. Scheme of keratin network assembly in WT keratinocytes and alterations in mutant cells examined in this study. The middle column depicts the known steps of keratin network morphogenesis. Yellow bars mark the steps affected in mutant cells, the cytoplasmic network alterations of which are shown at left and right. KtyII$^{-/-}$ keratinocytes incapable of synthesizing keratin type II polypeptides degrade unpaired type I keratins. Introduction of T150D K5 YFP into KtyII$^{-/-}$ cells allows formation of tetramers but impairs further assembly preventing keratin network formation. However, filament networks are still formed in the presence of endogenous WT type II keratins which, however, are coupled with cytoplasmic granule formation. T150A K5 YFP leads to increased bundling and reduced branching in KtyII$^{-/-}$ cells. K, keratin; KtyII, basal epidermal keratin type II; WT, wild type.

2017; Herrmann and Aebi, 2016)). The lateral packing of eight tetramers into the lattice generating the ULF, however, likely involves tighter contact of these regions. As shown in this study, introduction of a phosphomimetic residue at T150 of the K5 head efficiently impedes this process and subsequent assembly steps. The scheme further emphasizes the exponentially increasing tightness of intercalating ULF ends upon longitudinal annealing into keratin filament precursors. This is likely linked to close approximation of keratin polypeptide end domains, which may possibly bulge out from the filament surface. The occasional presence of small granular and elongated particles in T150D K5 YFP-producing KtyII$^{-/-}$ cells may indicate that ULF and keratin filament precursor formation still occur, albeit at very low efficiency and only in cells producing high levels of the mutant polypeptide. Granule formation in wild-type keratinocytes synthesizing T150D K5 YFP can be taken as further evidence for an inhibitory effect of the phosphomimetic mutant on filament formation. Phosphomimetic T150 mutation of K5 may also be linked to inhibition of filament bundling and branching as evidenced by network rarefication in these cells. On the other hand, we could show that T150A mutation increased filament bundling, branching, and stability. Taken together, T150 phosphorylation of K5 impairs keratin filament network assembly and, conversely, favors disassembly of keratin filaments.

We were surprised to find that a single phosphorylation site in a single keratin polypeptide was sufficient to completely prevent KF network formation given the large number of phosphorylation sites within individual keratins, the large number of kinases/phosphatases affecting keratin phosphorylation, the heteropolymeric nature of keratins, and the complexity of phenotypes reported so far and observed in this study for keratin phosphomutants. The use of keratin type II-depleted keratinocytes was crucial for uncovering the central functions of T150 in the type II keratin 5.

The results provide provocative ideas about EBS pathogenesis. They suggest that increased keratin phosphorylation is not only a consequence of keratin mutation but may actively influence disease progression through its effects on KF network formation, keratin turnover, and stress-induced signaling. It will be interesting to find out how the disease phenotype is affected by inhibiting/modulating T150 phosphorylation. This could be accomplished by inhibiting p38 MAPK, ERK1, or CK1, which likely target T150 (see Supplementary Figure S2).

MATERIALS AND METHODS

Antibodies

Polyclonal guinea pig antibodies against K5 and pan-keratin were obtained from PROGEN (Heidelberg, Germany), monoclonal mouse antibody directed against the LLpS/TPL motif recognizing the T150 K5 phosphoepitope (LJ4) was from Bishr Omary (Toivola et al., 2002), and polyclonal rabbit antibodies against K14 were recently described (Homberg et al., 2015). Polyclonal rabbit antibodies against phospho-histone H3, p38MAPK, phospho-p38MAPK, ERK, phospho-ERK, JNK, and phospho-JNK were from Cell Signaling (Danvers, MA). The secondary antibodies conjugated to horseradish peroxidase or fluorochromes were from Dianova (Hamburg, Germany).

DNA cloning

Preparation of cDNA constructs for fluorescence-tagged WT K5 and K8 and details on generating phosphorylation mutants are described in the Supplementary Materials and Methods online (see also Supplementary Tables S1 and S2 online).

Cell culture

The following cell lines were used in this study: human immortalized HaCaT cells (Boukamp et al., 1988); murine WT and KtyII$^{-/-}$ keratinocytes (Kroger et al., 2013); human epidermis-derived EBDM-4 keratinocytes from a patient with generalized severe EBS and control hKC keratinocytes from a healthy individual. The latter two cell lines were generated by E6/E7-mediated immortalization using a retroviral plxsn vector (Halbert et al., 1992) encoding E6/E7 and containing a G418 cassette for selection. Details on growth, passaging, transfection, clonal selection, MTT viability assay, and oxidative stress protocols are provided in Supplementary Materials and Methods.

Biochemical assays

Biochemical analyses, including cell fractionation, immunoblotting, co-immunoprecipitation, chemical crosslinking, sucrose gradient centrifugation, and mass spectrometry, are provided in the Supplementary Materials and Methods.

Statistical analysis

Prism 5 software (GraphPad, San Diego, CA) was used for statistical analysis. Comparison between two samples was performed with unpaired *t* test when data showed Gaussian distribution and Mann-Whitney test when otherwise. More than two sample groups were analyzed by one-way analysis of variance by Kruskal-Wallis test followed by Dunn posttest.

CONFLICT OF INTEREST

The authors state no conflict of interest.

ACKNOWLEDGMENTS

We thank Bishr Omary and Harald Herrmann for generously providing reagents. We also gratefully acknowledge the expert technical assistance of Ursula Wilhelm and Christiane Jaeschke. The work was supported by the Deutsche Forschungsgemeinschaft (LE566/18-1).

SUPPLEMENTARY MATERIAL

Supplementary material is linked to the online version of the paper at www.jidonline.org, and at https://doi.org/10.1016/j.jid.2017.10.011.

REFERENCES

Anton-Lamprecht I. Ultrastructural identification of basic abnormalities as clues to genetic disorders of the epidermis. J Invest Dermatol 1994;103(5 Suppl.):6S–12S.

Beriault DR, Haddad O, McCuaig JV, Robinson ZJ, Russell D, Lane EB, et al. The mechanical behavior of mutant K14-R125P keratin bundles and networks in NEB-1 keratinocytes. PLoS One 2012;7(2):e31320.

Boukamp P, Petrussevska RT, Breitkreutz D, Hornung J, Markham A, Fusenig NE. Normal keratinization in a spontaneously immortalized aneuploid human keratinocyte cell line. J Cell Biol 1988;106:761–71.

Chamcheu JC, Navsaria H, Pihl-Lundin I, Liovic M, Vahlquist A, Torma H. Chemical chaperones protect epidermolysis bullosa simplex keratinocytes from heat stress-induced keratin aggregation: involvement of heat shock proteins and MAP kinases. J Invest Dermatol 2011;131:1684–91.

Chou CF, Riopel CL, Rott LS, Omary MB. A significant soluble keratin fraction in 'simple' epithelial cells. Lack of an apparent phosphorylation and glycosylation role in keratin solubility. J Cell Sci 1993;105(Pt. 2):433–44.

Coulombe PA, Lee CH. Defining keratin protein function in skin epithelia: epidermolysis bullosa simplex and its aftermath. J Invest Dermatol 2012;132(3 Pt. 2):763–75.

Deek J, Hecht F, Rossetti L, Wissmiller K, Bausch AR. Mechanics of soft epithelial keratin networks depend on modular filament assembly kinetics. Acta Biomater 2016;43:218–29.

Dross N, Spriet C, Zwerger M, Muller G, Waldeck W, Langowski J. Mapping eGFP oligomer mobility in living cell nuclei. PLoS One 2009;4(4):e5041.

Elson EL, Magde D. Fluorescence correlation spectroscopy. I. Conceptual basis and theory. Biopolymers 1974;13:1–27.

Feng L, Zhou X, Liao J, Omary MB. Pervanadate-mediated tyrosine phosphorylation of keratins 8 and 19 via a p38 mitogen-activated protein kinase-dependent pathway. J Cell Sci 1999;112(Pt. 13):2081–90.

Fine JD, Bruckner-Tuderman L, Eady RA, Bauer EA, Bauer JW, Has C, et al. Inherited epidermolysis bullosa: updated recommendations on diagnosis and classification. J Am Acad Dermatol 2014;70:1103–26.

Gilmartin ME, Culbertson VB, Freedberg IM. Phosphorylation of epidermal keratins. J Invest Dermatol 1980;75:211–6.

Guldiken N, Zhou Q, Kucukoglu O, Rehm M, Levada K, Gross A, et al. Human keratin 8 variants promote mouse acetaminophen hepatotoxicity coupled with c-jun amino-terminal kinase activation and protein adduct formation. Hepatology 2015;62:876–86.

Guzenko D, Chernyatina AA, Strelkov SV. Crystallographic studies of intermediate filament proteins. Subcell Biochem 2017;82:151–70.

Halbert CL, Demers GW, Galloway DA. The E6 and E7 genes of human papillomavirus type 6 have weak immortalizing activity in human epithelial cells. J Virol 1992;66:2125–34.

Hatzfeld M, Burba M. Function of type I and type II keratin head domains: their role in dimer, tetramer and filament formation. J Cell Sci 1994;107(Pt. 7):1959–72.

Herrmann H, Aebi U. Intermediate filaments: structure and assembly. Cold Spring Harb Perspect Biol 2016;8(11):a018242.

Herrmann H, Häner M, Brettel M, Ku N, Aebi U. Characterization of distinct early assembly units of different intermediate filament proteins. J Mol Biol 1999;286:1403–20.

Herrmann H, Wedig T, Porter RM, Lane EB, Aebi U. Characterization of early assembly intermediates of recombinant human keratins. J Struct Biol 2002;137(1–2):82–96.

Homberg M, Magin TM. Beyond expectations: novel insights into epidermal keratin function and regulation. Int Rev Cell Mol Biol 2014;311:265–306.

Homberg M, Ramms L, Schwarz N, Dreissen G, Leube RE, Merkel R, et al. Distinct impact of two keratin mutations causing epidermolysis bullosa simplex on keratinocyte adhesion and stiffness. J Invest Dermatol 2015;135:2437–45.

Ikai K, McGuire JS. Phosphorylation of keratin polypeptides. Biochim Biophys Acta 1983;760:371–6.

Krieger JW, Singh AP, Bag N, Garbe CS, Saunders TE, Langowski J, et al. Imaging fluorescence (cross-) correlation spectroscopy in live cells and organisms. Nat Protoc 2015;10:1948–74.

Kroger C, Loschke F, Schwarz N, Windoffer R, Leube RE, Magin TM. Keratins control intercellular adhesion involving PKC-alpha-mediated desmoplakin phosphorylation. J Cell Biol 2013;201:681–92.

Ku NO, Michie SA, Soetikno RM, Resurreccion EZ, Broome RL, Omary MB. Mutation of a major keratin phosphorylation site predisposes to hepatotoxic injury in transgenic mice. J Cell Biol 1998;143:2023–32.

Liao J, Ku NO, Omary MB. Stress, apoptosis, and mitosis induce phosphorylation of human keratin 8 at Ser-73 in tissues and cultured cells. J Biol Chem 1997;272:17565–73.

Liao J, Lowthert LA, Ku NO, Fernandez R, Omary MB. Dynamics of human keratin 18 phosphorylation: polarized distribution of phosphorylated keratins in simple epithelial tissues. J Cell Biol 1995;131:1291–301.

Liao J, Omary MB. 14-3-3 proteins associate with phosphorylated simple epithelial keratins during cell cycle progression and act as a solubility cofactor. J Cell Biol 1996;133:345–57.

Lichtenstern T, Mücke N, Aebi U, Mauermann M, Herrmann H. Complex formation and kinetics of filament assembly exhibited by the simple epithelial keratins K8 and K18. J Struct Biol 2012;177(1):54–62.

Loffek S, Woll S, Hohfeld J, Leube RE, Has C, Bruckner-Tuderman L, et al. The ubiquitin ligase CHIP/STUB1 targets mutant keratins for degradation. Hum Mutat 2010;31:466–76.

Lopez CG, Saldanha O, Huber K, Köster S. Lateral association and elongation of vimentin intermediate filament proteins: A time-resolved light-scattering study. Proc Natl Acad Sci U S A 2016;113:11152–7.

Loschke F, Seltmann K, Bouameur JE, Magin TM. Regulation of keratin network organization. Curr Opin Cell Biol 2015;32:56–64.

Malhotra JD, Kaufman RJ. ER stress and its functional link to mitochondria: role in cell survival and death. Cold Spring Harb Perspect Biol 2011;3(9):a004424.

Morley SM, D'Alessandro M, Sexton C, Rugg EL, Navsaria H, Shemanko CS, et al. Generation and characterization of epidermolysis bullosa simplex cell lines: scratch assays show faster migration with disruptive keratin mutations. Br J Dermatol 2003;149:46–58.

Pan X, Hobbs RP, Coulombe PA. The expanding significance of keratin intermediate filaments in normal and diseased epithelia. Curr Opin Cell Biol 2013;25:47–56.

Planko L, Böhse K, Höhfeld J, Betz RC, Hanneken S, Eigelshoven S, et al. Identification of a keratin-associated protein with a putative role in vesicle transport. Eur J Cell Biol 2007;86:827–39.

Quinlan RA, Hatzfeld M, Franke WW, Lustig A, Schulthess T, Engel J. Characterization of dimer subunits of intermediate filament proteins. J Mol Biol 1986;192:337–49.

Russell D, Andrews PD, James J, Lane EB. Mechanical stress induces profound remodelling of keratin filaments and cell junctions in epidermolysis bullosa simplex keratinocytes. J Cell Sci 2004;117(Pt. 22):5233–43.

Sawant MS, Leube RE. Consequences of keratin phosphorylation for cytoskeletal organization and epithelial functions. Int Rev Cell Molec Biol 2017;330:171–225.

Senft D, Ronai ZA. UPR, autophagy, and mitochondria crosstalk underlies the ER stress response. Trends Biochem Sci 2015;40:141–8.

Snider NT, Omary MB. Post-translational modifications of intermediate filament proteins: mechanisms and functions. Nat Rev Mol Cell Biol 2014;15:163–77.

Steinert PM. The dynamic phosphorylation of the human intermediate filament keratin 1 chain. J Biol Chem 1988;263:13333–9.

Stumptner C, Omary MB, Fickert P, Denk H, Zatloukal K. Hepatocyte cytokeratins are hyperphosphorylated at multiple sites in human alcoholic hepatitis and in a mallory body mouse model. Am J Pathol 2000;156:77–90.

Sun G, Guo SM, Teh C, Korzh V, Bathe M, Wohland T. Bayesian model selection applied to the analysis of fluorescence correlation spectroscopy data of fluorescent proteins in vitro and in vivo. Anal Chem 2015;87:4326–33.

Szeverenyi I, Cassidy AJ, Chung CW, Lee BT, Common JE, Ogg SC, et al. The Human Intermediate Filament Database: comprehensive information on a gene family involved in many human diseases. Hum Mutat 2008;29:351–60.

Toivola DM, Zhou Q, English LS, Omary MB. Type II keratins are phosphorylated on a unique motif during stress and mitosis in tissues and cultured cells. Mol Biol Cell 2002;13:1857–70.

Wagner M, Trost A, Hintner H, Bauer JW, Onder K. Imbalance of intermediate filament component keratin 14 contributes to increased stress signalling in epidermolysis bullosa simplex. Exp Dermatol 2013;22:292–4.

Wally V, Lettner T, Peking P, Peckl-Schmid D, Murauer EM, Hainzl S, et al. The pathogenetic role of IL-1beta in severe epidermolysis bullosa simplex. J Invest Dermatol 2013;133:1901–3.

Werner NS, Windoffer R, Strnad P, Grund C, Leube RE, Magin TM. Epidermolysis bullosa simplex-type mutations alter the dynamics of the keratin cytoskeleton and reveal a contribution of actin to the transport of keratin subunits. Mol Biol Cell 2004;15:990–1002.

Wilson AK, Coulombe PA, Fuchs E. The roles of K5 and K14 head, tail, and R/K L E G E domains in keratin filament assembly in vitro. J Cell Biol 1992;119:401–14.

Windoffer R, Beil M, Magin TM, Leube RE. Cytoskeleton in motion: the dynamics of keratin intermediate filaments in epithelia. J Cell Biol 2011;194:669–78.

Wohland T, Shi X, Sankaran J, Stelzer EH. Single plane illumination fluorescence correlation spectroscopy (SPIM-FCS) probes inhomogeneous three-dimensional environments. Opt Express 2010;18:10627–41.

Woll S, Windoffer R, Leube RE. p38 MAPK-dependent shaping of the keratin cytoskeleton in cultured cells. J Cell Biol 2007;177:795–807.

Yano T, Tokui T, Nishi Y, Nishizawa K, Shibata M, Kikuchi K, et al. Phosphorylation of keratin intermediate filaments by protein kinase C, by calmodulin-dependent protein kinase and by cAMP-dependent protein kinase. Eur J Biochem 1991;197:281–90.

Zatloukal K, Stumptner C, Lehner M, Denk H, Baribault H, Eshkind LG, et al. Cytokeratin 8 protects from hepatotoxicity, and its ratio to cytokeratin 18 determines the ability of hepatocytes to form Mallory bodies. Am J Pathol 2000;156:1263–74.

Zhou Q, Cadrin M, Herrmann H, Chen CH, Chalkley RJ, Burlingame AL, et al. Keratin 20 serine 13 phosphorylation is a stress and intestinal goblet cell marker. J Biol Chem 2006;281:16453–61.